

# First-principles calculations for the elastic properties of Ni-base model superalloys: Ni/Ni<sub>3</sub>Al multilayers\*

Wang Yun-Jiang(王云江)<sup>†</sup> and Wang Chong-Yu(王崇愚)

Department of Physics, Tsinghua University, Beijing 100084, China

(Received 28 March 2009; revised manuscript received 3 April 2009)

A model system consisting of Ni[001](100)/Ni<sub>3</sub>Al[001](100) multi-layers are studied using the density functional theory in order to explore the elastic properties of single crystal Ni-based superalloys. Simulation results are consistent with the experimental observation that rafted Ni-base superalloys virtually possess a cubic symmetry. The convergence of the elastic properties with respect to the thickness of the multilayers are tested by a series of multilayers from 2 $\gamma'$ +2 $\gamma$  to 10 $\gamma'$ +10 $\gamma$  atomic layers. The elastic properties are found to vary little with the increase of the multilayer's thickness. A Ni/Ni<sub>3</sub>Al multilayer with 10 $\gamma'$ +10 $\gamma$  atomic layers (3.54 nm) can be used to simulate the mechanical properties of Ni-base model superalloys. Our calculated elastic constants, bulk modulus, orientation-dependent shear modulus and Young's modulus, as well as the Zener anisotropy factor are all compatible with the measured results of Ni-base model superalloys R1 and the advanced commercial superalloys TMS-26, CMSX-4 at a low temperature. The mechanical properties as a function of the  $\gamma'$  phase volume fraction are calculated by varying the proportion of the  $\gamma$  and  $\gamma'$  phase in the multilayers. Besides, the mechanical properties of two-phase Ni/Ni<sub>3</sub>Al multilayer can be well predicted by the Voigt-Reuss-Hill rule of mixtures.

**Keywords:** Ni-based superalloys, Ni/Ni<sub>3</sub>Al multilayer, mechanical property, first principles, rule of mixture

**PACC:** 4630, 6220D, 7115A

doi:10.1088/1674-1056/18/10/041

## 1. Introduction

Ni-base single-crystal (SC) superalloys are widely used for turbine blades and vanes in modern aero-engines as promising high-temperature structural materials because of their remarkable mechanical properties.<sup>[1]</sup> The typical microstructure of such superalloys is a high volume fraction of cuboidal  $\gamma'$  phase (L1<sub>2</sub>, ordered FCC, Ni<sub>3</sub>Al based) precipitates coherently embedded in the matrix  $\gamma$  phase (disordered FCC, solid solution based on Ni). The system is constituted by the two phases in which only phase interfaces appear. The  $\gamma$  and  $\gamma'$  phases are coherent with a simple cube-cube [001]||[001] relation.<sup>[2]</sup> They share a common Bravais lattice in their alignment. During the early stages of creep, the microstructure changes into a morphology called a rafted (directional coarsening) structure, namely a lamellar structure composed of  $\gamma$  and  $\gamma'$  phases alternately.<sup>[3,4]</sup> The rafted structure effectively impedes the dislocations movement through a variety of mechanisms by the  $\gamma/\gamma'$  interfaces, which provide a remarkable creep strength of Ni-base superalloys.<sup>[5-7]</sup>

The elastic constants are important for a basic

understanding of the excellent mechanical properties of the Ni-base superalloys. The elastic constants and the orientation-dependent elastic moduli of certain advanced nickel-base superalloys and model alloys have been measured previously by various methods.<sup>[8-13]</sup> However, the elastic properties of the rafted structure are not really understood from a theoretical view of point, especially in the framework of the precise quantum mechanics study. The rafted lamellar structure macroscopically possesses tetragonal elastic symmetry. It has a  $D_{4h}$  crystallographic point group. However, Ichitsubo *et al*<sup>[8,9]</sup> pointed out that the rafted superalloys virtually possess a cubic elastic symmetry even at room temperature. The reason is that the  $\gamma$  and  $\gamma'$  phases have similar elastic constants.

The precipitation of the large volume fraction (VF)  $\gamma'$  phase creates a large amount of interfacial area in the advanced nickel-base superalloys. The interfaces between  $\gamma$  and  $\gamma'$  phases play a critical role in the mechanical performance of the alloys. However, the investigation on the role of the interfaces in the elastic properties of the Ni-base superalloys is rare. On the other hand, the nickel-base superalloys are two-phase materials. The elastic properties of multi-

\*Project supported by the State Key Development Program for Basic Research of China (Grant No 2006CB605102).

<sup>†</sup>Corresponding author. E-mail: wangyunjiang05@mails.tsinghua.edu.cn

phase materials are often derived from its constitute phases by the rule of mixtures (ROM). The ROM is related to the volume fraction of the second phase. However, previous work in this field is usually on ceramic-metal composites by experiment.<sup>[14]</sup> Little has been done to the two-phase  $\gamma/\gamma'$  Ni-base superalloys.<sup>[10,15]</sup> For a more fundamental understanding of the mechanical behaviors of Ni-base superalloys, more effort should be made in this interesting field. Because the first-principle methods have been a great success in the studies of the strength of material<sup>[16–19]</sup> and the interface systems,<sup>[20–22]</sup> we apply a density functional theory (DFT) approach in order to provide reliable data to understand the elastic properties of Ni/Ni<sub>3</sub>Al multilayer systems, namely the Ni-base SC superalloys.

The objective of this work is to provide a better understanding of the elastic properties of Ni/Ni<sub>3</sub>Al multilayers as model Ni-base SC superalloys. As a first step, the macroscopical symmetry of the Ni/Ni<sub>3</sub>Al multilayers are determined by calculating the six independent elastic constants of the tetragonal multilayer at 0 K. Then we calculate the elastic properties of a series of periodic Ni/Ni<sub>3</sub>Al multilayers with different thicknesses. The purpose is to judge the thickness of the multilayers that can be regarded as a model Ni-base superalloy with both  $\gamma$  and  $\gamma'$  phases. Based on the determined thickness of the multilayers, the calculated elastic constants, the orientation-dependent elastic moduli (shear modulus  $G$  and Young's modulus  $E$ ) and the Zener anisotropy factor  $A$  of the Ni/Ni<sub>3</sub>Al multilayers are provided. The results are compared with the experiments. Finally the volume fractions of the  $\gamma'$  phase are changed from 40% to 80% in multilayers, and the elastic properties are also provided. The results are fitted by the rule of mixtures related to the two-phase alloys. A comparison of the fitted elastic properties for bulk Ni and bulk Ni<sub>3</sub>Al with the direct first-principle results are made. The results provide a concrete sight into the mechanical properties of Ni-based SC superalloys from a theoretical view of point.

## 2. Method and computational model

The first-principle calculations presented here are based on the electronic density-functional theory (DFT), and have been carried out by using the

*ab initio* program VASP.<sup>[23]</sup> The generalized gradient approximation (GGA) of projector augmented wave (PAW)<sup>[24]</sup> is adopted for parametrization of the exchange-correlation function. The cut-off energy of atomic wave functions is set to be 350 eV. In the present work, the set of  $k$  points is chosen according to the size of the computational cell with a regular Monkhorst-Pack grid of special  $k$ -point. All the internal freedoms of the multilayers supercell models are relaxed. The break condition for the electronic self-consistent and ionic relaxation are  $10^{-4}$  eV and  $10^{-3}$  eV, respectively. The calculation of total energy is followed by cell optimization with stopping criterion for electronic convergence of  $10^{-5}$  eV.

The elastic constants are evaluated by means of the total energies calculated as a function of suitable applied stains.<sup>[25]</sup> The energy density is fitted by a polynomial, and its second derivative at the equilibrium volume is determined.

A series of Ni[001](100)||Ni<sub>3</sub>Al[001](100) multilayers with different thicknesses and a volume proportion of two phases are constructed as Ni-base model superalloys in our study. The lateral lattice parameter for both  $\gamma$  Ni and  $\gamma'$  Ni<sub>3</sub>Al is the same for the coherence assumption. The multilayers are modeled by periodic slabs with  $m$  the number of atomic layers Ni<sub>3</sub>Al(100) and  $n$  the number of atomic layers Ni(100). The (100) layers are periodically stacking as shown in Fig.1. Figures 1(a) and 1(b) are the conventional unit cells of FCC Ni and L1<sub>2</sub> Ni<sub>3</sub>Al. Figure 1(c) is the smallest  $2\gamma' + 2\gamma$  atomic layers Ni/Ni<sub>3</sub>Al multilayer, which contains only one Ni<sub>3</sub>Al unit cell and one Ni unit cell.

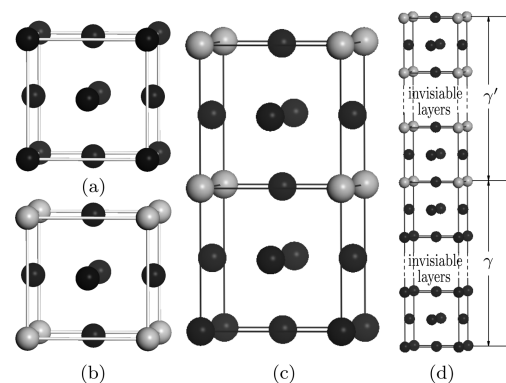


**Fig.1.** (a) Conventional unit cell of FCC Ni, (b) unit cell of L1<sub>2</sub> Ni<sub>3</sub>Al, (c) the smallest periodically repeated blocks of 2+2 layers Ni/Ni<sub>3</sub>Al(100) multilayer and (d) schematics of the  $m+n$  layers periodically repeated Ni/Ni<sub>3</sub>Al(100) multilayers. The black and grey atoms are Ni and Al atoms, respectively.

Figure 1(d) is the schematics of the  $m\gamma' + n\gamma$  atomic layers Ni/Ni<sub>3</sub>Al multilayers used in our calculations.

There are  $m/2$  Ni<sub>3</sub>Al unit cells and  $n/2$  Ni unit cells altogether in the  $m\gamma' + n\gamma$  atomic layers multilayers. For testing the convergency of elastic properties with respect to the thickness of the multilayers, the number  $m$  is set to be equal to  $n$ .

### 3. Results and discussion

#### 3.1. The symmetry of Ni-base superalloys

The rafted Ni-base superalloys are thought to possess macroscopically tetragonal elastic symmetry. However, previous experimental studies have shown that at low temperature the rafted structure virtually possesses a simple cubic symmetry.<sup>[8,9]</sup> The tetragonal  $D_{4h}$  crystal has six independent elastic constants:  $C_{11}$ ,  $C_{33}$ ,  $C_{12}$ ,  $C_{13}$ ,  $C_{44}$  and  $C_{66}$ . For the more symmetric cubic crystal the non-zero independent elastic constants are reduced to  $C_{11}$ ,  $C_{12}$  and  $C_{44}$ , where  $C_{11} = C_{33}$ ,  $C_{12} = C_{13}$ , and  $C_{44} = C_{66}$ . As a first step, the elastic symmetry of the tetragonal Ni/Ni<sub>3</sub>Al multilayer is determined by calculation of the six independent elastic constants.

In order to calculate the elastic constants of the multilayer, the theoretical equilibrium volume  $V_0$  of the supercell is firstly determined by fitting the total energies versus volume according to the Murnaghan equation of state.<sup>[26]</sup> The elastic energy density of a solid under small strain is given by

$$\frac{\Delta E}{V_0} = \frac{1}{2} \sum_{i=1}^6 \sum_{j=1}^6 C_{ij} e_i e_j, \quad (1)$$

where  $V_0$  is the equilibrium volume of the undistorted lattice cell,  $\Delta E$  is the energy increment from the strain with strain vector  $\epsilon = (e_1, e_2, e_3, e_4, e_5, e_6)$ . In order to calculate the six elastic constants of the tetragonal Ni/Ni<sub>3</sub>Al multilayer, we apply an appropriate set of distortions with the distortion parameter  $\delta$  from  $-0.03$  to  $0.03$  in the step of  $0.005$ . The applied strain configurations and the energy-strain relations are listed in Table 1. The calculated strain energy density is fitted to a polynomial in  $\delta$  and then equated to the appropriate elastic constants.

Table 2 lists the calculated six independent elastic constants of two Ni/Ni<sub>3</sub>Al multilayers. The small one contains  $2\gamma' + 2\gamma$  atomic layers and the large one contains  $10\gamma' + 10\gamma$  atomic layers. We can see from Table 2 that the elastic constants vary little from  $2\gamma' + 2\gamma$

to  $10\gamma' + 10\gamma$  atomic layers multilayers. For both multilayers, the elastic constant  $C_{11}$  is very close to  $C_{33}$ ,  $C_{12}$  is nearly equal to  $C_{13}$  and  $C_{44}$  differs very little from  $C_{66}$ . Take the more reliable  $10\gamma' + 10\gamma$  atomic layers multilayer for example, the values of the ratios are  $C_{11}/C_{33} = 0.9761$ ,  $C_{12}/C_{13} = 0.9982$ ,  $C_{44}/C_{66} = 1.0113$ . Because our first-principle calculations are done at  $0$  K, we can conclude that the tetragonal Ni/Ni<sub>3</sub>Al multilayer virtually possesses a more symmetric cubic symmetry at a low temperature. Thus we confirm the pervious experimental results from Ichitsubo *et al.*<sup>[8,9]</sup> Based on this, we can take the Ni/Ni<sub>3</sub>Al multilayer (which is modeled as Ni-base superalloys) as a cubic symmetry crystal in the next Section.

**Table 1.** The six applied strain configurations used to calculate the six independent elastic constants of tetragonal Ni/Ni<sub>3</sub>Al multilayers.

	strain configuration	energy-strain relation
1	$\epsilon = (\delta, 0, 0, 0, 0, 0)$	$\Delta E/V_0 = \frac{1}{2} C_{11} \delta^2$
2	$\epsilon = (\delta, \delta, 0, 0, 0, 0)$	$\Delta E/V_0 = (C_{11} + C_{12}) \delta^2$
3	$\epsilon = (0, 0, \delta, 0, 0, 0)$	$\Delta E/V_0 = \frac{1}{2} C_{33} \delta^2$
4	$\epsilon = (\delta, 0, \delta, 0, 0, 0)$	$\Delta E/V_0 = \frac{1}{2} (C_{11} + 2C_{13} + C_{33}) \delta^2$
5	$\epsilon = (0, 0, 0, \delta, 0, 0)$	$\Delta E/V_0 = \frac{1}{2} C_{44} \delta^2$
6	$\epsilon = (0, 0, 0, 0, \delta, 0)$	$\Delta E/V_0 = \frac{1}{2} C_{66} \delta^2$

**Table 2.** Calculated values of the elastic constants ( $C_{ij}$  in GPa) of the 2+2, 10+10 layers Ni/Ni<sub>3</sub>Al multilayers.

	$C_{11}$	$C_{33}$	$C_{12}$	$C_{13}$	$C_{44}$	$C_{66}$
2+2	237.5	246.5	164.2	164.6	113.6	117.2
10+10	236.7	242.5	166.4	166.7	116.8	115.5

#### 3.2. The relation between mechanical properties and the thickness of Ni/Ni<sub>3</sub>Al multilayers

The purpose of this work is to study the mechanical properties of Ni-base superalloys by using the Ni/Ni<sub>3</sub>Al multilayers. To the limit of first-principle method, the multilayers supercell cannot be large enough to be the size of real  $\gamma/\gamma'$  superalloys. As a result, the convergency of the mechanical properties with respect to the multilayer thickness has to be tested. In this part, the tetragonal Ni/Ni<sub>3</sub>Al multilayer is regarded to possess a cubic symmetry. The three elastic constants together with bulk modulus

$B$ , shear modulus  $G$ , Young's modulus  $E$ ,  $G/B$  ratio, Poisson ratio  $\nu$  and Zener anisotropy factor  $A$  are calculated as a function of thickness of the Ni/Ni<sub>3</sub>Al multilayer. In order to test the convergency, the  $m\gamma' + n\gamma$  multilayers shown in Fig.1(d) are varying from  $2\gamma' + 2\gamma$  to  $10\gamma' + 10\gamma$  atomic layers with  $m = n$ . Correspondingly, the thickness of the multilayers is varying from 7.08 Å to 35.4 Å (1 Å = 0.1 nm).

For the cubic symmetry, there are three independent elastic constants  $C_{11}$ ,  $C_{12}$  and  $C_{44}$ . In order to obtain them, the theoretical equilibrium volume  $V_0$  and bulk modulus  $B$  are determined by fitting the total energies versus volume according to the Murnaghan equation of state.<sup>[26]</sup> The cubic shear constants  $C' = (C_{11} - C_{12})/2$  and  $C_{44}$  are determined by applying an appropriate set of distortions with the distortion parameter  $\delta$  from -0.06 to 0.06 in the step of 0.01. The applied strain configurations  $\epsilon$  and the corresponding strain-energy density variations  $\Delta E/V_0$  to  $\delta$  are shown in Table 3. Relaxation of the internal degrees of freedom is carried out in the case of all strained crystals.

**Table 3.** The two applied strain configurations used to calculate shear constant  $C' = \frac{1}{2}(C_{11} - C_{12})$  and  $C_{44}$  of cubic Ni/Ni<sub>3</sub>Al multilayers.

	strain configuration	energy-strain relation
1	$\epsilon = (\delta, \delta, (1+\delta)^{-2}-1, 0, 0, 0)$	$\Delta E/V_0 = 6C'\delta^2 + O(\delta^3)$
2	$\epsilon = (0, 0, 0, \delta, \delta, \delta)$	$\Delta E/V_0 = \frac{3}{2}C_{44}\delta^2$

The elastic constants are calculated using the Hill averaging method.<sup>[27]</sup> First, the  $C_{11}$  and  $C_{12}$

elastic constants are separated from the bulk modulus  $B = \frac{1}{3}(C_{11} + 2C_{12})$  and the shear constant  $C'$ . Then, the shear modulus is calculated as the arithmetic Hill average  $G = \frac{1}{2}(G_V + G_R)$ , where  $G_V = (C_{11} - C_{12} + 3C_{44})/5$  and  $G_R = 5/(4S_{11} - 4S_{12} + 3S_{44})$  are the Voigt and Reuss bounds, respectively, and  $S_{11}$ ,  $S_{12}$ , and  $S_{44}$  are the elastic compliances.<sup>[28]</sup> Finally, the Young's modulus  $E$  and Poisson ratio  $\nu$  are obtained as  $E = 9GB/(G + 3B)$  and  $\nu = \frac{1}{2} \left( \frac{3B - 2G}{3B + G} \right)$ , respectively. Besides, the Zener anisotropy factor  $A = 2C_{44}/(C_{11} - C_{12})$ .

The calculated values of mechanical parameters for Ni/Ni<sub>3</sub>Al multilayers from  $2\gamma' + 2\gamma$  atomic layers to  $10\gamma' + 10\gamma$  atomic layers are summarized in Table 4. It is noted that the parameters vary little from the  $2\gamma' + 2\gamma$  multilayer to  $10\gamma' + 10\gamma$  multilayer. This means that the mechanical parameters depend little on the thickness of the multilayers. The proportion of the two phases in the multilayer is related more to the mechanical behaviors, which can be seen in the following study. Based on our study, the  $10\gamma' + 10\gamma$  atomic layers (35.4 Å thick) multilayer is thick enough for the simulation of the Ni-base model alloys. Since the first-principles calculations for these large systems are very time-consuming, we use the  $m\gamma' + n\gamma$  ( $m + n = 20$ ) atomic layers Ni/Ni<sub>3</sub>Al multilayers as the Ni-base model superalloys. The number of atomic layers  $m$  and  $n$  are varied in the following study to change the volume fraction of strengthening phase  $\gamma'$ -Ni<sub>3</sub>Al.

**Table 4.** Calculated values of the elastic constants ( $C_{ij}$  in GPa), bulk modulus ( $B$  in GPa), shear modulus ( $G$  in GPa), Young's modulus ( $E$  in GPa),  $G/B$  ratio, Poisson ratio  $\nu$  and anisotropy factor  $A$  of the  $n + n$  layers Ni/Ni<sub>3</sub>Al multilayers.

	$C_{11}$	$C_{12}$	$C_{44}$	$B$	$G$	$E$	$G/B$	$\nu$	$A$
2+2	243.3	158.1	114.1	186.5	76.9	202.8	0.41	0.319	2.68
4+4	242.9	159.1	115.1	187.0	76.8	202.6	0.41	0.319	2.75
6+6	242.5	159.1	114.8	186.9	76.5	202.0	0.41	0.320	2.75
8+8	241.5	159.5	113.1	186.8	75.3	199.2	0.40	0.322	2.76
10+10	242.4	159.0	114.9	186.8	76.6	202.1	0.41	0.320	2.76

### 3.3. A comparison with the experimental results

In order to verify the validity of our method for the calculations of mechanical parameters for the Ni-base model alloys, the calculated results are compared with the experimental observations. The compared mechanical properties contain elastic constants  $C_{ij}$ , bulk modulus  $B$ , orientation-dependent shear modulus  $G$  and Young's modulus  $E$ , and anisotropy factor  $A$ .

The orientation-dependent elastic moduli  $E$  and  $G$  are related to the elastic compliances through the following expressions:<sup>[10,29]</sup>

$$E(\theta, \varphi) = (S_{11} - 2SJ)^{-1}, \quad (2)$$

$$G(\theta, \varphi) = (S_{44} + 4SJ)^{-1}, \quad (3)$$

$$S = S_{11} - S_{12} - S_{44}/2, \quad (4)$$

$$J = \sin^2 \theta \cdot \cos^2 \theta + 0.125 \cdot \sin^4 \theta (1 - \cos 4\varphi), \quad (5)$$

where  $E(\theta, \varphi)$  and  $G(\theta, \varphi)$  are the specific orientational Young's modulus and shear modulus.  $\theta$  and  $\varphi$  are the Eulerian angles.  $\theta$  is the angle between the specimen axis and the [001] crystal direction.  $\varphi$  is the angle between the specimen axis projection in the (001) plane and the [010] crystal direction. Here the

coupling effect correction between torsion and bending are neglected since the errors can be tolerant in our calculation.

The advanced commercial Ni-base superalloys have a high volume fraction of  $\gamma'$ -Ni<sub>3</sub>Al phase. For the comparison between our results with the experimental ones, we calculate the mechanical properties of the three multilayers with different  $\gamma'$  volume fractions. Those are the multilayers with  $10\gamma' + 10\gamma$ ,  $12\gamma' + 8\gamma$  and  $14\gamma' + 6\gamma$  atomic layers, representing 50%, 60% and 70%  $\gamma'$  phase volume fractions, respectively. The calculated values and the experimental results for several typical superalloys are summarized in Table 5. The Young's modulus and shear modulus for three orientations [100], [110] and [111] are included.

**Table 5.** Calculated values of the elastic constants ( $C_{ij}$  in GPa), bulk modulus ( $B$  in GPa), orientation-dependent shear modulus ( $G$  in GPa) and Young's modulus ( $E$  in GPa), and the anisotropy factor  $A$  of the  $m+n$  layers Ni/Ni<sub>3</sub>Al multilayers with different Ni<sub>3</sub>Al volume fractions (VF). The experimental values of typical Ni-based superalloys are also listed for comparison.

	$\gamma'$ -VF	$C_{11}$	$C_{12}$	$C_{44}$	$B$	$G[100]$	$G[110]$	$G[111]$	$E[100]$	$E[110]$	$E[111]$	$A$
this work	50%	242.4	159.0	114.9	186.8	114.9	61.2	54.8	116.4	209.7	262.2	2.76
	60%	239.8	157.2	115.6	184.7	115.6	60.9	54.4	115.3	209.7	262.5	2.80
	70%	238.3	155.1	116.1	182.8	116.1	61.3	54.8	116.0	209.7	263.1	2.79
R1 <sup>a</sup>	47%								116	208	283	2.76
TMS-26 <sup>b</sup>	60%	252.5	158.5	131.8	189.0				130.6			
TMS-26 <sup>c</sup>		251.4	160.1	129.4					126.8			
CMSX-4 <sup>d</sup>	60%	251	159	132		127	66	57	124	226	311	2.87
CMSX-4 <sup>e</sup>									128	226	313	2.85
CMSX-4 <sup>f</sup>									127.6	227.9		

<sup>a</sup> Ref.[10], <sup>b</sup> Ref.[8], <sup>c</sup> Ref.[9], <sup>d</sup> Ref.[11], <sup>e</sup> Ref.[10], <sup>f</sup> Ref.[13]

The mechanical properties of the listed experiments are measured at room temperature. R1 is a model Ni-base superalloy with only 0.9 wt.% alloying element Mo, which has the most similar chemical composition to our model alloys. The  $\gamma'$  phase volume fraction is 47%. Our calculated orientation-dependent Young's modulus and Zener anisotropy factor of the 50% VF  $\gamma'$  phase multilayer are in excellent agreement with that of the R1 model alloys.  $E[100]$ ,  $E[110]$  and  $A$  are perfectly consistent with the experimental results measured for R1. All the three differences between our calculations and the experiments are within 0.8%. The calculated  $E[111]$  are 7.35% smaller than the experimental value. The reason is that there exists no alloying elements in our Ni-base

model alloys: Ni/Ni<sub>3</sub>Al multilayer. The same trend can be seen from the difference of  $E[111]$  between model alloy R1 and the commercial Ni-base superalloys CMSX-4.<sup>[10,11]</sup> The value for  $E[111]$  obviously increases from R1 to CMSX-4 because there are more alloying elements in the latter. This illustrates that  $E[111]$  depends strongly upon the amount of alloying elements in the superalloys. Besides the model alloys R1, the elastic properties of commercial superalloys TMS-26 and CMSX-4 are also compared with our results. The volume fractions of the  $\gamma'$  phase in these superalloys are approximately 60%. Therefore we make a contrast with the  $12\gamma' + 8\gamma$  multilayer. It is pleasant to find that our calculated values are similar to the experimental ones. Especially the elas-

tic  $C_{12}$ , bulk modulus  $B$ , shear modulus  $G$ [111] and anisotropy factor  $A$  which are very consistent. The values for our calculated 60% VF  $\gamma'$  phase multilayer are only a little lower than the modulus of TMS-26 or CMSX-4. For our calculation, the rest mechanical parameters are smaller than that of advanced commercial Ni-base superalloys. This may be related to the fact that our Ni-base model superalloys (the multilayers) contain no alloying elements. In summary, our calculations successfully derive the mechanical properties of Ni-base superalloys. The results compare well with the experimental elastic properties of the Ni-base model alloy R1 and advanced commercial Ni-base superalloys TMS-26 and CMSX-4.

### 3.4. The mechanical properties as function of Ni<sub>3</sub>Al phase volume fraction

#### 3.4.1. The coherent lattice parameters

All the Ni/Ni<sub>3</sub>Al interface multilayers in our study are coherent, for which the lateral parameters for both Ni and Ni<sub>3</sub>Al are the same. In order to simulate the mechanical properties of the Ni-base model superalloys with different volume fractions, we firstly determined the equilibrium configuration for the multilayers by the Murnaghan equation of state.<sup>[26]</sup> The multilayers are  $8\gamma' + 12\gamma$ ,  $10\gamma' + 10\gamma$ ,  $12\gamma' + 8\gamma$  and  $14\gamma' + 6\gamma$  and  $16\gamma' + 4\gamma$ , representing 40%, 50%, 60%, 70% and 80%  $\gamma'$  VF, respectively. For the sake of comparison, we also calculated the lattice parameters for pure Ni and pure Ni<sub>3</sub>Al. The results are  $a_\gamma = 3.515 \text{ \AA}$  and  $a_{\gamma'} = 3.568 \text{ \AA}$ , which are consistent with the experimental measurements.<sup>[30,31]</sup> The lattice parameters of the coherent Ni/Ni<sub>3</sub>Al multilayers as a function of the  $\gamma'$  VF are shown in Fig.2. Because the lattice parameter of Ni<sub>3</sub>Al is bigger than that of Ni, the coherent lattice parameter of the multilayer increases with the increase of  $\gamma'$ -Ni<sub>3</sub>Al VF. All the coherent lattice parameters of multilayers with 40%–80% VF Ni<sub>3</sub>Al ( $V_p$ ) are fitted to the following linear equation:

$$a_0(V_p) = 3.515 + 0.053 \cdot V_p \text{ (\AA)}. \quad (6)$$

We can see from Fig.2 that it is a very good fit. All the lattice parameters of coherent multilayers with different  $\gamma'$  VF lie right on the line. When  $V_p = 0$  and  $V_p = 1$ , the lattice parameters with the first-principles calculated and experimental ones for the pure Ni and Ni<sub>3</sub>Al are perfectly retrieved.

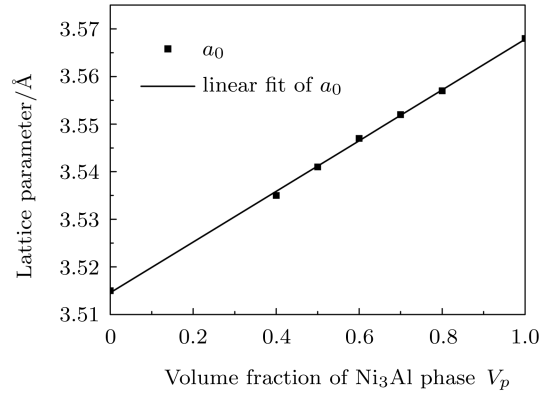


**Fig.2.** The lattice parameters of the coherent Ni[001]/Ni<sub>3</sub>Al[001] multilayers as a function of Ni<sub>3</sub>Al volume fraction. The solid line is the linear fit.

#### 3.4.2. The elastic constants

The elastic properties of multi-phase materials are usually related to their constitute single phases by the rule of mixtures (ROM). The first order ROM corresponds to simple averaging concepts like the formulae of Voigt,<sup>[29]</sup> Reuss<sup>[32]</sup> and Hill<sup>[27]</sup> (VRH). More exact descriptions of the elastic properties of a multi-phase material are summarized in Ref.[14], in which the volume fraction, shape, orientation, and orientation distribution of a second phase are taken into consideration. Kuhn *et al*<sup>[15]</sup> pointed out that VRH-rules are good approximation for the most Ni-base superalloys. The difference between VRH and other higher order ROMs is within 1%. Thus the VRH-rules are used for our study on the mechanical properties of the Ni-base model superalloys as a function of Ni<sub>3</sub>Al phase VF.

The mean value of the serial (Voigt, iso-stress) and parallel (Reuss, iso-strain) arrangement of two constitute phases proposed by Hill are given as follows:

$$K_c = \frac{1}{2} \left( K_m V_m + K_p V_p + \frac{K_m K_p}{K_m V_p + K_p V_m} \right), \quad (7)$$

where  $K_c$  are the elastic properties of a two-phase material ( $C_{ij}$ ,  $E$ ,  $G$ ,  $\nu$ ),  $K_m$  and  $K_p$  are the elastic properties of the matrix and the precipitates, respectively.  $V_m$  and  $V_p$  are the VF of the matrix and the precipitates ( $V_m + V_p = 1$ ), respectively.

Figures 3-5 are the plots of elastic constants  $C_{ij}$  as a function of the VF of Ni<sub>3</sub>Al phase. It can be seen that  $C_{11}$  and  $C_{12}$  decrease with the increase of  $V_p$ . Whereas  $C_{44}$  increases with the increase of  $V_p$ . These are consistent with the fact that  $C_{11}$  and  $C_{12}$  of  $\gamma'$ -Ni<sub>3</sub>Al are smaller than that of  $\gamma$ -Ni, while  $C_{44}$  of  $\gamma'$  is bigger than that of  $\gamma$ . We also apply the VRH-ROM

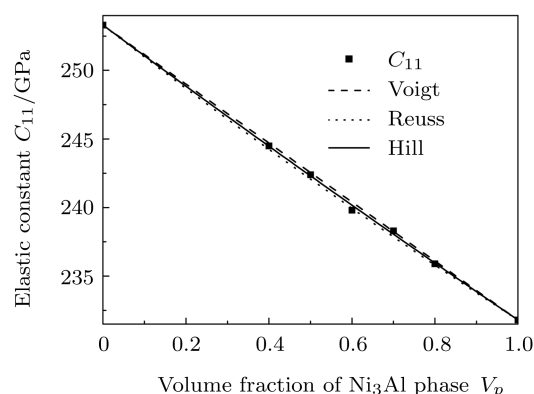


**Fig.3.** The elastic constant  $C_{11}$  of the Ni[001]/Ni<sub>3</sub>Al[001] multilayers as a function of Ni<sub>3</sub>Al volume fraction. The solid line is the fit of Hill's mixture rule formula. The Voigt-Reuss bounds are also shown as the dashed and dotted lines.

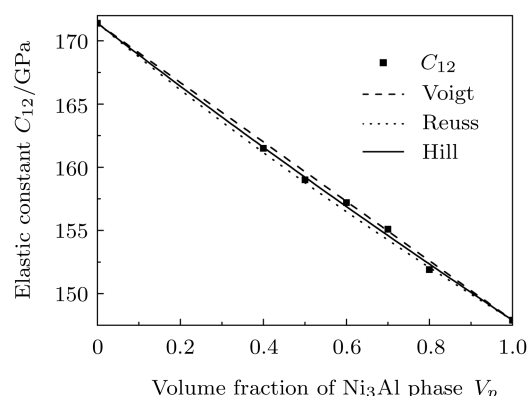


**Fig.4.** The elastic constant  $C_{12}$  of the Ni[001]/Ni<sub>3</sub>Al[001] multilayers as a function of Ni<sub>3</sub>Al volume fraction. The solid line is the fit of Hill's mixture rule formula. The Voigt-Reuss bounds are also shown as the dashed and dotted lines.

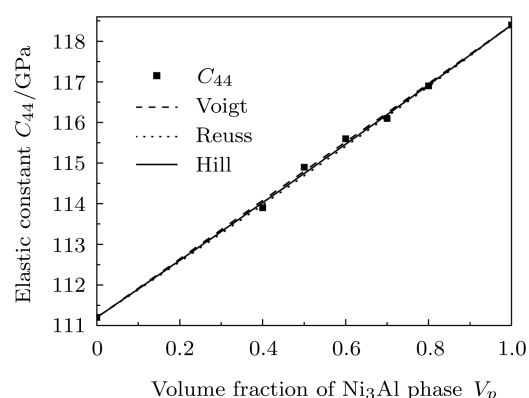


**Fig.5.** The elastic constant  $C_{44}$  of the Ni[001]/Ni<sub>3</sub>Al[001] multilayers as a function of Ni<sub>3</sub>Al volume fraction. The solid line is the fit of Hill's mixture rule formula. The Voigt-Reuss bounds are also shown as the dashed and dotted lines.

to the calculated values. The calculated elastic constants  $C_{ij}$  of the Ni/Ni<sub>3</sub>Al multilayers with  $V_p$  from

40% to 80% are fitted to the ROM formula (7) by the solid line shown in Figs.3-5. The Voigt-Reuss bounds are also shown as the dashed and dotted lines. It is pleasant to see that nearly all the data are within the frame work of RVH rules. Based on our results, we can say that VRH-ROM is a very good method to predict the elastic constants of the two-phase Ni-base superalloys. It is suitable for the two-phase superalloys with small difference in the elastic properties of  $\gamma$  and  $\gamma'$ .

### 3.4.3. The elastic moduli

The bulk modulus  $B$ , shear modulus  $G$  and Young's modulus  $E$  of Ni/Ni<sub>3</sub>Al multilayers as functions of  $V_p$  are shown in Figs.6-8. It is also noted that  $B$  ( $G$ ,  $E$ ) decreases (increase) with the increase of  $V_p$ . These behaviors are obvious because the modulus  $B$  of Ni is bigger than that of Ni<sub>3</sub>Al, while  $E$  and  $G$  *vice versa*. As the lines in the figures for the elastic constants, the VRH rule of mixture is also applied to the elastic moduli. It is interesting to find that the bulk modulus  $B$  is well within the framework of Voigt-Reuss bounds. However, most of the data for  $E$  and  $G$  are scattered. One reason for the failure of VRH mixture rules is that the values of  $E$  and  $G$  in this part are calculated using the Hill averaging method.<sup>[27]</sup> That is the arithmetic average of the iso-strain and iso-stress bounds, not the orientation-dependent  $E$  and  $G$ . Therefore the average values of up and low bounds of elastic moduli cannot always be described by the VRH rules of mixtures. The other one is that the moduli of Ni and Ni<sub>3</sub>Al are too close to each other. Thus the Voigt, Reuss and Hill formulas are nearly equal, the differences between the fit results

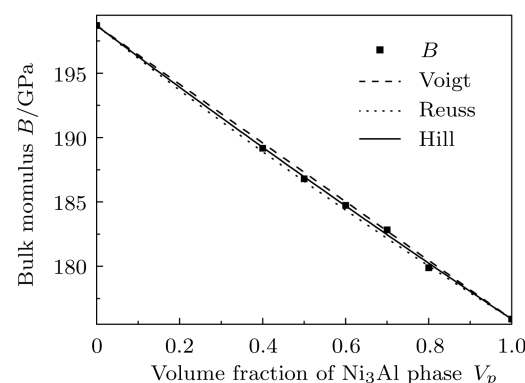


**Fig.6.** The bulk modulus  $B$  of the Ni[001]/Ni<sub>3</sub>Al[001] multilayers as a function of Ni<sub>3</sub>Al volume fraction. The solid line is the fit of Hill's mixture rule formula. The Voigt-Reuss bounds are also shown as the dashed and dotted lines.

and the calculated values are magnified in Figs.7 and 8.

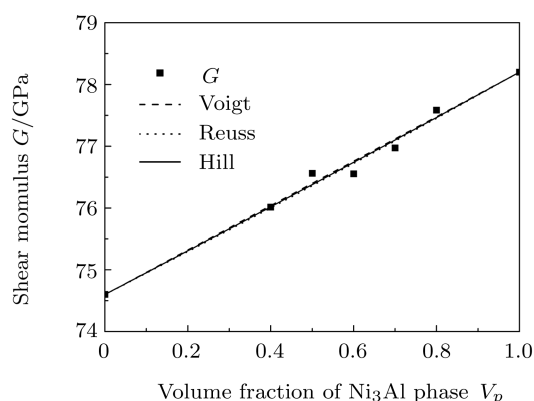


**Fig.7.** The shear modulus  $G$  of the Ni[001]/Ni<sub>3</sub>Al[001] multilayers as a function of Ni<sub>3</sub>Al volume fraction. The solid line is the fit of Hill's mixture rule formula. The Voigt-Reuss bounds are also shown as the dashed and dotted lines.

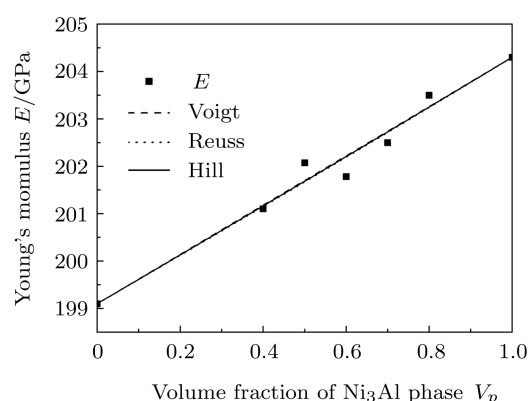


**Fig.8.** The Young's modulus  $E$  of the Ni[001]/Ni<sub>3</sub>Al[001] multilayers as a function of Ni<sub>3</sub>Al volume fraction. The solid line is the fit of Hill's mixture rule formula. The Voigt-Reuss bounds are also shown as the dashed and dotted lines.

### 3.4.4. The ductile/brittle behaviors

According to Pugh's empirical rule,<sup>[33]</sup> the ductile/brittle behaviors of material are closely related to the ratio of  $G/B$  or Poisson ratio  $\nu$ . A high value of  $G/B$  and low value of  $\nu$  is associated with brittleness. The increase in  $G/B$  or decrease in  $\nu$  indicates a decrease in ductility. Figures 9 and 10 are the  $G/B$  ratio and Poisson ratio  $\nu$  of Ni/Ni<sub>3</sub>Al multilayers as functions of  $V_p$ . It is interesting to note that  $G/B$  ( $\nu$ ) is increasing (decreasing) with the increase of  $\gamma'$  volume fraction. These behaviors of  $G/B$  ( $\nu$ ) illustrate that the Ni-base model superalloys are becoming more brittle when the volume fraction of  $\gamma'$  phase is increasing. This is consistent with the fact that Ni<sub>3</sub>Al is more brittle than Ni. Besides the ductile/brittle analysis, we also attempt to fit the  $G/B$  and  $\nu$  with different  $V_p$  by using the VRH-ROM. We are enlightened to

find that VRH formula fits the ductile/brittle behaviors well. The  $G/B$  and  $\nu$  values all lie within the Voigt-Reuss bounds.

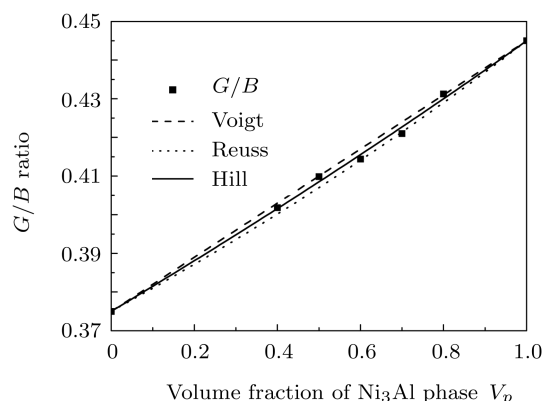


**Fig.9.** The  $G/B$  ratio of the Ni[001]/Ni<sub>3</sub>Al[001] multilayers as a function of Ni<sub>3</sub>Al volume fraction. The solid line is the fit of Hill's mixture rule formula. The Voigt-Reuss bounds are also shown as the dashed and dotted lines.

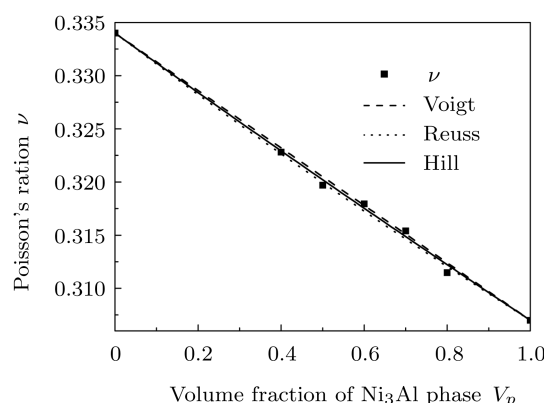


**Fig.10.** The Poisson ratio of the Ni[001]/Ni<sub>3</sub>Al[001] multilayers as a function of Ni<sub>3</sub>Al volume fraction. The solid line is the fit of Hill's mixture rule formula. The Voigt-Reuss bounds are also shown as the dashed and dotted lines.

When  $V_p$  are 0 and 1, which means that the Ni/Ni<sub>3</sub>Al multilayers are changing to the pure Ni and pure Ni<sub>3</sub>Al. Thus the VRH formula fitted by the data with 40%-80%  $\gamma'$  volume fraction can predict the elastic properties precisely for the pure Ni and pure Ni<sub>3</sub>Al. In order to verify the validity of VRH-ROM to the Ni-base model superalloys (the Ni/Ni<sub>3</sub>Al multilayer), we list the results of direct first-principles (FP) calculated elastic properties as well as the VRH-ROM prediction in Table 6. Their differences are also included. We can see from the table that the VRH results are quite the same as the direct FP values. The biggest difference appears in  $C_{11}$  of Ni with only a 1.7%. The comparison again agrees with our point that VRH rule of mixture is suitable for the Ni-base model superalloys.



**Table 6.** Comparison of the direct first principles (FP) calculated values of the elastic constants ( $C_{ij}$  in GPa), bulk modulus ( $B$  in GPa), shear modulus ( $G$  in GPa), Young's modulus ( $E$  in GPa),  $G/B$  ratio, Poisson ratio of the bulk Ni and bulk Ni<sub>3</sub>Al to the fit results of Voigt-Reuss-Hill's rule of mixture. Their differences are also listed.

		$C_{11}$	$C_{12}$	$C_{44}$	$B$	$G$	$E$	$G/B$	$\nu$
Ni	FP	249.0	168.8	111.3	195.9	73.9	197.0	0.378	0.332
	VRH-fit	253.3	171.4	111.2	198.7	74.6	199.1	0.375	0.334
	diff.	+1.7%	+1.5%	-0.1%	+1.6%	+0.9%	+1.1%	-0.8%	+0.6%
Ni <sub>3</sub> Al	FP	231.3	149.9	119.9	177.0	77.8	203.6	0.440	0.308
	VRH-fit	231.8	147.9	118.4	175.9	78.2	204.3	0.445	0.307
	diff.	+0.2%	-1.3%	-1.3%	-0.6%	+0.5%	+0.3%	+1.1%	-0.3%

## 4. Summary

We perform a first-principles study on the mechanical properties of Ni[001](100)/Ni<sub>3</sub>Al[001](100) multilayer as an Ni-base model superalloys. In summary, the following conclusions can be drawn.

(i) The symmetry of the rafted Ni-base superalloys are determined by calculations of the six independent elastic constants of the tetragonal crystal. We find that for both the  $2\gamma' + 2\gamma$  and  $10\gamma' + 10\gamma$  atomic multilayers, the elastic constant  $C_{11}$  is very close to  $C_{33}$ ,  $C_{12}$  is nearly equal to  $C_{13}$  and  $C_{44}$  and differs very little from  $C_{66}$ . The more reliable  $10\gamma' + 10\gamma$  multilayer gives the values of the ratios  $C_{11}/C_{33} = 0.9761$ ,  $C_{12}/C_{13} = 0.9982$ ,  $C_{44}/C_{66} = 1.0113$ . Thus the Ni/Ni<sub>3</sub>Al multilayer (the Ni-base model superalloys) virtually possesses a more symmetric cubic symmetry at low temperature, which is consistent with the ultrasonics measurements of elastic constants from Ichit-subo *et al.*<sup>[8,9]</sup>

(ii) The convergence of the mechanical properties with respect to the thickness of the Ni/Ni<sub>3</sub>Al multilayer is tested. The elastic constants, bulk modulus, Hill's average moduli,  $G/B$  ratio, Poisson ratio and Zener anisotropy factor of multilayers with  $2\gamma' + 2\gamma$  to  $10\gamma' + 10\gamma$  atomic layers are determined. We find that these elastic properties vary little with the increased thickness of a multilayer. The  $10\gamma' + 10\gamma$  multilayer with a thickness of 35.4 Å is reliable enough for the simulation of the mechanical properties of Ni-base model superalloys.

(iii) In order to validate our method, we calculated the elastic properties of the 35.4 Å Ni/Ni<sub>3</sub>Al multilayers. The volume fractions of  $\gamma'$ -Ni<sub>3</sub>Al are 50%, 60% and 70%, which are comparable with those

of the experimental Ni-base superalloys. The elastic properties contain elastic constants  $C_{ij}$ , bulk modulus  $B$ , orientation-dependent shear modulus  $G$  and Young's modulus  $E$ , as well as the anisotropy factor  $A$ . Our calculated orientation-dependent Young's modulus  $E$  and anisotropy factor  $A$  are in excellent agreement with the experimental R1 Ni-base model alloys at room temperature.<sup>[10]</sup> The reason is that the compositions of R1 are very close to our model alloys. We also compare our results with different  $\gamma'$  VF to the advanced commercial Ni-base superalloys TMS-26<sup>[8,9]</sup> and CMSX-4<sup>[10,11,13]</sup> at low temperature. The calculated values are also quite consistent to the experimental ones with different measurement techniques. It is also interesting to note that our calculated values are consistently smaller than the experimental ones of commercial superalloys. The reason is obviously because in commercial alloys, many alloying elements are added, which is effectively strengthening the superalloys.

(iv) The lattice parameters of the coherent Ni/Ni<sub>3</sub>Al multilayers are derived from the Murnaghan equation of state.<sup>[26]</sup> We find a very good linear relation between the coherent lattice parameters and VF of  $\gamma'$ -Ni<sub>3</sub>Al precipitate phase. The linear equation is:

$$a_0(V_p) = 3.515 + 0.053 \cdot V_p \quad (\text{\AA}).$$

(v) The mechanical properties of the Ni/Ni<sub>3</sub>Al multilayer are calculated as a function of the  $\gamma'$ -Ni<sub>3</sub>Al volume fraction. We find that  $C_{11}$ ,  $C_{12}$ ,  $B$  and  $\nu$  are decreasing with the increase of Ni<sub>3</sub>Al phase VF. This is consistent with the fact that these properties of the pure Ni are larger than those of the pure Ni<sub>3</sub>Al. While the behaviors of  $C_{44}$ ,  $G$ ,  $E$  and  $G/B$  ratio as functions of  $V_p$  are different, they all decrease with the increas-

ing of  $V_p$ . Based on the  $G/B$  and  $\nu$  ratios, we can say that the Ni/Ni<sub>3</sub>Al multilayer becomes more brittle with the increase of  $V_p$ . Because the Ni<sub>3</sub>Al phase is more brittle than Ni. Besides the above study, we apply the VRH-ROM to the mechanical properties of multilayers with 40%–80%  $\gamma'$  VF. The data are fitted well to the VRH rule of the mixture shown in formula (7). The Voigt and Reuss bounds are also shown. The elastic properties of the two-phase  $\gamma$ – $\gamma'$  alloys are well

depicted by the VRH rules of mixtures.

## Acknowledgements

The authors wish to thank Dr. T. Ichitsubo for providing experimental data on TMS-26 by resonance ultrasound spectroscopy (RUS) measurements and his helpful discussions.

## References

- [1] Sims C T 1987 *Superalloy II* (New York: Wiley) pp97–131
- [2] Kear B K and Pope D P 1989 In: Tien J K and Caufield T ed., *Superalloy, Super-composites and Superceramics* (Boston, MA: Academic Press) pp564
- [3] Pollock T M and Argon A S *Acta Metall. Mater.* **42** 1895
- [4] Epishin A, Link T, Portela P D and Brückner U *Acta Mater.* **48** 4169
- [5] Pearson D D, Lemkey F D and Kear B H 1980 *Superalloys* (The Minerals, Metals & Materials Society) p513
- [6] Harada H, Ohno K, Yamagata T, Yokokawa T and Yamazaki M 1988 *Superalloys* (The Minerals, Metals & Materials Society) p513
- [7] Tien J K and Gamble R P 1972 *Metall. Trans.* **3** 2157
- [8] Ichitsubo T, Ogi H, Hirao M, Tanaka K, Osawa M, Yokokawa T, Kobayashi T and Harada H 2002 *Ultrasonics* **40** 211
- [9] Ichitsubo T, Koumoto D, Hirao M, Tanaka K, Osawa M, Yokokawa T and Harada H 2003 *Acta Mater.* **51** 4863
- [10] Fährmann M, Hermann W, Fährmann E, Boegli A, Pollock T M and Sockel H G 1999 *Mater. Sci. Eng. A* **260** 212
- [11] Zhang X, Stoddart P R, Comins J D and Every A G 2001 *J. Phys.: Condes. Matter* **13** 2281
- [12] Kuo C M 2007 *Mater. Sci. Eng. A* **494** 103
- [13] Sawant A and Tin S 2008 *Scripta Mater.* **58** 275
- [14] Hsieh C L and Tuan W H 2005 *Mater. Sci. Eng. A* **393** 133
- [15] Kuhn H A and Sockel H G 1990 *Phys. Stat. Sol. (a)* **119** 93
- [16] Šob M, Friák M, Legut D, Fiala J and Vitek V 2004 *Mater. Sci. Eng. A* **387–389** 148
- [17] Liu Z J, Qi J H, Guo Y, Chen Q F, Cai L C and Yang X D 2007 *Chin. Phys.* **16** 499
- [18] Zhu J, Yu J X, Wang Y J, Chen X R and Jing F Q 2008 *Chin. Phys. B* **17** 2216
- [19] Yao Q, Xing H and Sun J 2006 *Appl. Phys. Lett.* **89** 161906
- [20] Wang S Q and Ye H Q 2006 *Curr. Opin. Solid State Mat. Sci.* **10** 26
- [21] Lazar P, Redinger J and Podloucky R 2007 *Phys. Rev. B* **76** 174112
- [22] Wang S W, Gudipati R, Rao A S, Bostelmann T H and Shen Y G 2007 *Appl. Phys. Lett.* **91** 081916
- [23] Kresse G and Hafner J 1993 *Phys. Rev. B* **48** 13115
- [24] Kresse G and Joubert J 1999 *Phys. Rev. B* **59** 1758
- [25] Wang S Q and Ye H Q 2003 *J. Phys.: Condes. Matter* **15** 5307
- [26] Murnaghan F D 1994 *Proc. Natl. Acad. Sci. U.S.A.* **30** 244
- [27] Hill R 1952 *Proc. Phys. Soc. London* **65** 349
- [28] Grimvall G 1999 *Thermophysical Properties of Materials* (Amsterdam: NorthHolland)
- [29] Voigt W 1928 *Lehrbuch der Kristallphysik* (Leipzig: Teubner)
- [30] Kittel C 1986 *Introduction to Solid State Physics* (New York: Wiley Interscience)
- [31] Yoo M H 1987 *Acta Metall.* **35** 1559
- [32] Reuss A and Angew Z 1929 *Math. Mech.* **9** 49
- [33] Pugh S F 1954 *Philos. Mag.* **45** 823